crystals

MDPI

Article

Intramolecularly Stabilized *o*-Carboranyl Aluminum Complexes: Synthesis, Characterization, and X-ray Structural Studies

Honglae Sohn and Jong-Dae Lee *

Department of Chemistry, College of Natural Sciences, Chosun University, Gwangju 61452, Republic of Korea
* Correspondence: jdlee@chosun.ac.kr

Abstract: The chelating aluminum complex [2-(Me_2NCH_2)$C_2B_{10}H_{10}$]AlX_2 (X = Br **3**, CH_3 **4**) was synthesized using 2-dimethylaminomethyl-*o*-carboranyl lithium ($LiCab^N$, **2**) with aluminum tribromide ($AlBr_3$) or dimethylaluminum bromide (Me_2AlBr), resulting in a modest yield. Compound **4** was obtained by reacting compound **3** with methyllithium (CH_3Li) in toluene. All compounds were characterized using infrared (IR) spectroscopy; ^1H, ^{11}B, ^{13}C nuclear magnetic resonance (NMR) spectroscopy; and X-ray crystallography. X-ray structural studies of Cab^NAlBr_2 (**3**) and Cab^NAlMe_2 (**4**) (Cab^N = 2-dimethylaminomethyl-*o*-carboranyl) indicated that the aluminum atom was located at the center of a distorted tetrahedron. Crystal structures of Cab^NAlBr_2 (**3**) [a = 8.9360(3) Å, b = 12.0358(9) Å, c = 14.7730(4) Å, $\alpha = \beta = \gamma = 90°$] and Cab^NAlMe_2 (**4**) [a = 8.9551(3) Å, b = 11.9126(9) Å, c = 14.7711(4) Å, $\alpha = \beta = \gamma = 90°$] were obtained. The reactivity of aluminum complexes **3** and **4** with Lewis bases, such as H_2O, pyridine, alkylamines, and arylamines, confirmed their rapid decomposition due to the strong Lewis acidity of aluminum metals.

Keywords: C,N-chelate ligand; 2-dimethylaminomethyl-*o*-carborane; organoaluminum complexes; X-ray crystallography; intramolecularly coordination

Citation: Sohn, H.; Lee, J.-D. Intramolecularly Stabilized *o*-Carboranyl Aluminum Complexes: Synthesis, Characterization, and X-ray Structural Studies. *Crystals* **2023**, *13*, 877. https://doi.org/10.3390/cryst13060877

Academic Editor: Yulia V. Nelyubina

Received: 24 April 2023
Revised: 24 May 2023
Accepted: 25 May 2023
Published: 27 May 2023

1. Introduction

Organometallic compounds with unique properties and specific reactivities can be prepared by utilizing the properties of C,N-chelating ligands [1]. These properties derive from the extension of their coordination number via the intramolecular coordination of a C,N-chelating ligand. Various organoaluminum compounds with C,N-chelating ligands have been prepared for the purpose of bonding to aluminum atoms via Al–C covalent bonds and Al–N dative bonds [2–12]. Recently, interest in aluminum nitride (AlN) [13], a form in which aluminum and nitrogen are combined, has been on the rise due to AlN being one of the few materials with both a wide direct bandgap and large thermal conductivity [14–20]. Group 13 metal nitrides are commonly used in optoelectronics [21–26], as well as in high-power and high-frequency electronics [27–31], owing to their small atomic mass, strong interatomic bonds, and simple crystal structure [32]. In particular, from among group 13 metal nitrides, AlN has the highest thermal conductivity and demonstrates the most effective dissipation of heat from a wide variety of power and radio frequency electronics [27–31].

o-Carborane is a cluster compound of great interest owing to its ease of preparation and derivatization, thermal stability, and steric bulkiness [33]. Therefore, it was necessary to investigate the possibility of synthesizing intramolecular coordination complexes in a 2-dimethylaminomethyl-*o*-carboranyl ($HCab^N$, **1**) system. For these reasons, it is interesting to investigate the possibility of synthesizing such intramolecularly N-coordinated aluminum metal complexes using the potentially bidentate ligand system [34,35].

This study reports on the synthesis, characterization, and X-ray structural study of organoaluminum complexes of the type (Cab^N)AlX_2 (X = Br, CH_3), in which the alu-

minum metal center can be regarded as tetracoordinated because of intramolecular Al–N coordination. We have previously reported on the successful synthesis and structural characterization of tetracoordinated gallium complexes containing an N- or P-donor [34,36]. We observe from these results that N-donor, far more so than P-donor, ligand systems have a reduced probability of forming the desired intramolecular stabilization as the size of the incoming metal increases, that is, unless specific electronic factors intervene. In this respect, we have started to investigate the synthesis of intramolecularly stabilized aluminum metal complexes that bear a steric bulky o-carboranyl ligand system [33].

Thus, we report, in this paper, the detailed synthetic procedures of (*o*-carboranylamino) aluminum compounds and their complete characterization using IR, NMR spectroscopy, and X-ray diffraction. The preparation of this type of compound starts from the reaction of metal halides with (2-dimethylaminomethyl-*o*-carboranyl)lithium (**2**). Herein, we reported the appropriate synthetic procedures and spectroscopic characteristics of novel intramolecularly coordinated aluminum complexes and the reactivities of these compounds toward a Lewis base.

2. Materials and Methods

2.1. General Procedures

All manipulations were performed under a dry, oxygen-free nitrogen or argon atmosphere using standard Schlenk techniques Alternatively, they were conducted in vacuum conditions in a KK-011AS glove box. Ether and toluene were dried and distilled from sodium benzophenone. Hexane was dried and distilled over CaH_2. ^{1}H, ^{11}B, and ^{13}C NMR spectra were recorded on a JEOL 300 MHz NMR spectrometer as operating at 300.1, 96.3, and 75.4 MHz, respectively. All the boron-11 chemical shifts were referenced to $BF_3{\cdot}O(C_2H_5)_2$ (0.0 ppm), with a negative sign indicating an upfield shift. All proton and carbon chemical shifts were measured in relation to the internal residual benzene in the lock solvent (99.5% C_6D_6) and then referenced to tetramethylsilane (0.00 ppm). IR spectra were recorded using a Bio-Rad FTS-165 spectrophotometer. Elemental analyses were performed using a Carlo Erba Instruments CHNS-O EA1108 analyzer. All melting points were uncorrected. Decaborane and (dimethylamino)-2-propyne were purchased from Katchem and Aldrich, respectively, and used without purification. Cab^N (**1**; $HCab^N$, 2-[(dimethylamino)methyl]-*o*-carborane) [37] was prepared according to the specifications of a previously reported method. The starting material $AlBr_3$ was purchased from Strem Chemical and sublimed under dynamic vacuum conditions prior to each use. Dimethylaluminum bromide [38] was prepared by conducing stoichiometric ligand redistribution reactions in pentane at room temperature, after which it was purified by vacuum sublimation at room temperature.

2.2. X-ray Crystallography

Details of the crystal data and a summary of the intensity data collection parameters for **3** and **4** are provided in Table 1. Crystals of **3** and **4** were grown in a toluene solution and stored at −20 °C. They were then mounted in thin-walled glass capillaries, sealed under an argon atmosphere, and transferred to the goniometer of the Bruker SMART 1000 CCD area detector system. The initial unit cell parameters were obtained using the SMART [39] software. Data integration, correction for Lorentz and polarization effects, and final cell refinement were performed using SAINTPLUS [40]. The data were further corrected for absorption using SADABS [41]. The initial structure solutions were obtained via direct methods in SHELXTL [42]. Subsequent refinement cycles (based on F^2) and Fourier synthesis revealed the positions of all non-hydrogen atoms. The atoms were refined using anisotropic displacement tensors. All hydrogen atoms were added to the calculated positions for the final refinement cycle.

Table 1. X-ray crystallographic data and processing parameters for compounds **3** and **4**.

Identification code	KOR103	KOR106
Empirical formula	C_5 H_{18} B_{10} N_1 Br_2 Al_1	C_7 H_{24} B_{10} N_1 Al_1
Formula weight	387.08	257.37
Temperature	293(2) K	293(2) K
Wavelength	0.71073 Å	0.71073 Å
Crystal system, space group	Orthorhombic, *Cmc* 2_1	Orthorhombic, *Cmc* 2_1
Unit cell dimensions	a = 8.9360(3) Å, α = 90.00°	a = 8.9551(3) Å, α = 90.00°
	b = 12.0358(9) Å, β = 90.00°	b = 11.9126(9) Å, β = 90.00°
	c = 14.7730(4) Å, γ = 90.00°	c = 14.7711(4) Å, γ = 90.00°
Volume	1588.9(1) $Å^{-3}$	1575.8(1) $Å^{-3}$
Z, D_{calc}	4, 1.618 g/cm^3	4, 1.085 g/cm^3
Absorption coefficient	5.132 mm^{-1}	0.153 mm^{-1}
F(000)	752	544
Crystal size	0.2 × 0.16 × 0.14 mm	0.18 × 0.14 × 0.10 mm
θ range for data collection	2.76 to 25.97°	2.76 to 25.95°
Limiting indices	$-8 \leq h \leq 10$, $-8 \leq k \leq 14$, $-18 \leq l \leq 0$	-8 h ≤ 11, $-8 \leq k \leq 14$, $-8 \leq 1 \leq 18$
Reflections collected/unique	1693/853 [R(int) = 0.0891]	1748/845 [R(int) = 0.0703]
Completeness to θ = 25.96	99.9%	100.0%
Refinement method	Full-matrix least-squares on F^2	Full-matrix least-squares on F^2
Data/restraints/parameters	853/1/98	845/1/105
Goodness-of-fit on F^2	0.923	1.005
Final R indices [$I > 2\sigma$ (I)]	[a] R1 = 0.0394, [b] wR2 = 0.0834	[a] R1 = 0.0448, [b] wR2 = 0.1110
R indices (all data)	[a] R1 = 0.1020, [b] wR2 = 0.0881	[a] R1 = 0.0876, [b] wR2 = 0.1066
Extinction coefficient	0.19(3)	−0.3(6)
Largest diff. peak and hole	0.713 and −0.700 e·$Å^{-3}$	0.193 and −0.227 e·$Å^{-3}$

[a] $R_1 = \sum||F_o| - |F_c|| / \sum|F_o|$ (based on reflections with $F_o^2 > 2\sigma F^2$), [b] $wR_2 = [\sum[w(F_o^2 - F_c^2)^2] / \sum[w(F_o^2)^2]]^{1/2}$; $w = 1/[\sigma^2(F_o^2) + (0.095P)^2]$; and $P = [\max(F_o^2, 0) + 2F_c^2]/3$(also with $F_o^2 > 2\sigma F^2$)

*2.3. Synthesis of $Cab^N AlBr_2$ (**3**)*

We added 1.6 M *n*-BuLi (2 mL, 3.2 mmol) via a syringe to a stirred solution of Cab^N (**1**; 0.604 g, 3.0 mmol) in 30 mL of hexane, cooled to −10 °C. The resulting white suspension ($LiCab^N$, **2**) was stirred at −10 °C for 2 h and then transferred through a cannula to a suspension of $AlBr_3$ (0.80 g, 3.0 mmol) in 50 mL of toluene at −78 °C. The reaction temperature was first maintained at −78 °C for 1 h, after which the reaction mixture was slowly warmed to room temperature. After being stirred for an additional 12 h, the mixture was filtered. The solvent was removed under vacuum conditions, and the resulting residue was taken up in a minimum of toluene. This was then recrystallized by cooling the solution to −20 °C. Compound **3** was isolated from the reaction solution in 82% yield as colorless crystals (0.95 g, 2.5 mmol). Anal. Calcd: C, 15.51; H, 4.69; N, 3.62. Found: C, 15.71; H, 4.88; N, 3.72. MP: 231–232 °C. IR (Nujol, cm^{-1}): ν(C-H) 3100, 2990; ν(B-H) 2590. ^{1}H NMR (C_6D_6, 300.1 MHz) δ 1.630 (s, N–CH_3), 2.212 (s, N-CH_2). ^{11}B NMR (C_6D_6, 96.3 MHz) δ –2.31 (d, 1B, $J_{B\text{-}H}$ = 150 Hz), –4.08 (d, 1B, $J_{B\text{-}H}$ = 175 Hz), –5.79 (d, 2B, $J_{B\text{-}H}$ = 150 Hz), –9.72 (d, 1B, fulllength), –11.14 (d, 1B, $J_{B\text{-}H}$ = 125 Hz), −11.75 (d, 2B, fulllength), −12.95 (d, 2B, fulllength). ^{13}C NMR (C_6D_6, 75.4 MHz) δ 52.060 (N-CH_3), 66.517 (N-CH_2), 72.674 (*carborane*).

*2.4. Synthesis of $Cab^N AlMe_2$ (**4**)*

We added 1.6 M *n*-BuLi (2 mL, 3.2 mmol) via a syringe to a stirred solution of Cab^N (**1**; 0.604 g, 3.0 mmol) in 30 mL of hexane, cooled to −10 °C. The resulting white suspension ($LiCab^N$, **2**) was stirred at −10 °C for 2 h and then transferred through a cannula to a suspension of Me_2AlBr (0.41 g, 3.0 mmol) in 50 mL of toluene at −78 °C. The reaction temperature was first maintained at −78 °C for 1 h, after which the reaction mixture was slowly warmed to room temperature and it was observed that LiBr precipitation was produced from the solution. After being stirred for an additional 12 h, the mixture was filtered. The solvent was removed under vacuum conditions, and the resulting residue

was taken up in a minimum of toluene and then recrystallized by cooling the solution to −20 °C. Compound **4** was isolated from the reaction solution as colorless crystals with a 61% yield (0.47 g, 1.8 mmol). Anal. Calcd: C, 32.67; H, 9.40; N, 5.44. Found: C, 32.74; H, 9.53; N, 5.55. MP: 175–177 °C. IR (Nujol, cm^{-1}): ν(C-H) 3100, 2990; ν(B-H) 2590. ^{1}H NMR (C_6D_6, 300.1 MHz) δ 0.520 (s, Al-CH_3), 1.512 (s, N-CH_3), 2.087 (s, N-CH_2). ^{11}B NMR (C_6D_6, 400 MHz) δ −3.18 (d, 1B, $J_{B\text{-}H}$ = 155 Hz), −4.31 (d, 1B, $J_{B\text{-}H}$ = 137 Hz), −10.10 (d, 2B, $J_{B\text{-}H}$ = 170 Hz), −12.88 (d, 6B, $J_{B\text{-}H}$ = 135 Hz). ^{13}C NMR (C_6D_6, 75.4 MHz) δ 10.377 (Al-CH_3), 48.774 (N-CH_3), 63.124 (N-CH_2), 73.800 (*carborane*).

*2.5. Reaction of Cab^{N}AlBr$_2$ (**3**) with LiMe*

We added 1.4 M solution of LiMe in diethyl ether (1.6 mL, 2.2 mmol) to a stirred solution of **3** (0.77 g, 2.0 mmol) in toluene (30 mL) at −78 °C via a syringe. The reaction temperature was first maintained at −78 °C for 1 h, after which the reaction mixture was slowly warmed to room temperature. It was observed that LiBr precipitation was produced from the solution. After being stirred for 3 h, the mixture was filtered. The solvent was removed under vacuum conditions, and the resulting residue was taken up in a minimum of toluene and then recrystallized by cooling the solution to −20 °C. Compound **4** was isolated from the reaction solution in colorless crystals with a 20% yield (0.10 g, 0.40 mmol).

3. Results

*3.1. Synthesis of Cab^{N}AlBr$_2$ (**3**)*

As shown in Scheme 1, intramolecularly stabilized tetracoordinated 2-dimethylaminomethyl-*o*-carboranyl aluminum compound Cab^{N}AlBr$_2$ (**3**) was synthesized from aluminum tribromide with 2-dimethylaminomethyl-o-carboranyllithium (**2**) in toluene solvent. Compound **3** was stabilized by the formation of a five-membered ring with C,N-chelating ligand. Notably, compound **3** was moderately unstable in air and decomposed slowly upon contact with O_2 and moisture.

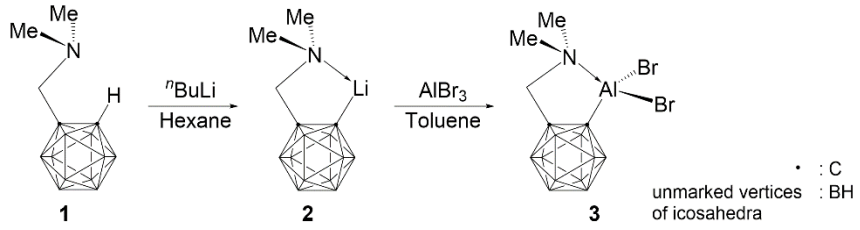

Scheme 1. Synthesis of Cab^{N}AlBr$_2$ (**3**).

It was confirmed that the synthesis and structures of compounds **3** and **4** showed a very similar story to the results obtained for gallium compounds that we have already reported [34]. Detailed information on the structural determinations of compounds **3** and **4** are provided Tables S1–S6 in the Supplementary Materials. Compound **3** was purified from colorless crystals via a process of low-temperature recrystallization in toluene. Satisfactory elemental analysis was performed for compound **3**. The structure of compound **3** was proposed based on the corresponding IR, ^{1}H, ^{11}B, and ^{13}C NMR spectroscopic data. Details of the crystal data and a summary of the intensity data collection parameters of compound **3** are provided in Tables 1 and 2, respectively. The Ortep diagram of compound **3**, shown in Figure 1, was determined via the use of single-crystal X-ray diffraction (XRD). The selected interatomic distances and angles are listed in Table 2. Similar to the results obtained in our previously published work,[34] the molecule lays on a crystallographic reflection plane and exhibited rigorously imposed reflection symmetry. Seven atoms, namely Al(1), N(1), C(13), C(2), C(1), B(9), and B(12), lay on the symmetry plane. The dimethylamine group of the *o*-carboranyl ligand was coordinated to the aluminum metal in **3**, resulting in the formation of a five-membered chelate ring, N(1)–Al(1)–C(1)–C(2)–C(13). The Al(1), Br(1), Br(1)*, and C(1) moieties were close to planar, with aluminum −0.532(4) Å above the

Br(1)Br(1)*C(1) plane. The angles around the aluminum metal center did not deviate much from the tetrahedral angle, except for the C(1)–Al(1)–N(1) angle in the five-membered ring, which was 92.2(4)°. This also influenced the geometry around the *o*-carborane cluster; the C(2)–C(1)–Al(1) angle (107.9(7)°) within the five-membered ring was similar to that expected at 108°. The Al(1)–N(1) distance in **3** (2.039(1) Å) was longer than that obtained in the corresponding amine-ligated aryl system [*o*-(Me_2NCH_2)C_6H_4]$AlBr_2$ (2.003(5) Å).[7] The Al(1)–N(1) distance of 2.039(1) Å was in agreement with the corresponding values observed in the adducts formed between AlX_3 and NR_3 [43–50]; all distances were longer than the sum of the covalent radii for aluminum and nitrogen (1.95 Å) [51]. The Al(1)–C(1) distance (1.938(1) Å) was similar to that reported for other organoaluminum compounds [6,7,52–55]. The Al–Br distance of 2.216(2) Å was within the range of typical covalent Al–Br bond distances (2.310–2.316 Å) [7].

Table 2. Selected interatomic distances (Å), angles, and torsion angles (°) for **3** and **4**.

Compound **3**			
Al1−C1	1.938(1)	Al1−N1	2.039(1)
Al1−Br1	2.216(2)	N1−C13	1.518(2)
Al1−Br#1	2.216(2)	N1–C14	1.476(1)
C1–C2	1.649(2)	N1–C#14	1.476(1)
C2–C13	1.516(2)		
C1−Al1−N1	92.2(4)	C13−N1−Al1	109.4(8)
C1−Al1−Br1	113.7(2)	C2−C1−Al1	107.9(7)
C1−Al1−Br#1	113.7(2)	Br#1−Al1−Br1	115.7(2)
N1−Al1−Br1	109.5(2)	C#14−N1−C14	108.6(1)
N1−Al1−Br#1	109.5(2)	C14–N1–C13	109.2(8)
Compound **4**			
Al1−C1	2.010(6)	Al1−N1	2.090(5)
Al1−C15	1.947(5)	N1−C13	1.507(7)
Al1−C#15	1.947(5)	N1–C14	1.488(5)
C1–C2	1.652(8)	N1–C#14	1.488(5)
C2–C13	1.532(8)		
C1−Al1−N1	88.4(2)	C13−N1−Al1	113.2(3)
C1−Al1−C15	113.1(2)	C2−C1−Al1	108.9(3)
C1−Al1−C#15	113.1(2)	C#15−Al1−C15	119.4(3)
N1−Al1−C15	109.1(2)	C#14−N1−C14	108.0(6)
N1−Al1−C#15	109.1(2)	C14–N1–C13	108.3(3)

Symmetry code: (i) x, y, z, (ii) −x, −y, z + 1/2, (iii) −x, y, z + 1/2, (iv) x, −y, z, (v) x + 1/2, y + 1/2, z, (vi) −x + 1/2, −y + 1/2, z + 1/2, (vii) −x + 1/2, y + 1/2, z + 1/2, (viii) x + 1/2, −y + 1/2, z.

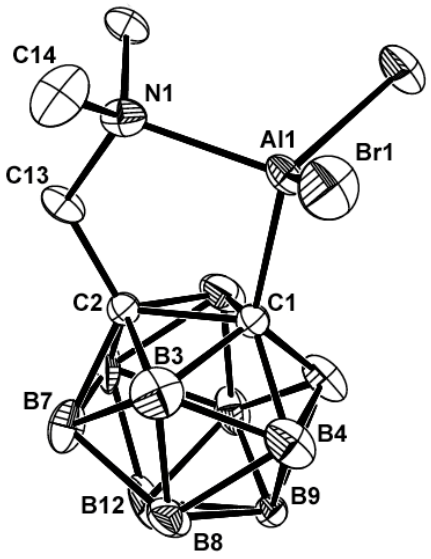

Figure 1. Molecular structure of Cab^NAlBr_2 (**3**). Thermal ellipsoids are drawn at the 30% probability level. (CCDC No. 2256552 in Appendix A).

3.2. Synthesis of $Cab^{N}AlMe_2$ (**4**)

As shown in Scheme 2, the intramolecularly coordinated 2-dimehylaminomethyl-*o*-carboranyl dimethylaluminum compound $Cab^{N}AlMe_2$ (**4**) was obtained from dimethylaluminum bromide and $LiCab^{N}$ (**2**). This compound also forms colorless crystals, demonstrates stability in an inert gas environment, and exhibits slow decomposition upon exposure to air. It is readily soluble in pentane, hexane, and aromatic solvents. Similar to compound **3**, IR, ^{1}H, ^{11}B, and ^{13}C NMR spectra exhibited the expected patterns and chemical shifts. The molecular structure of **4** was determined via the use of a single-crystal X-ray diffractometer (XRD). The structure is shown in Figure 2, and details of the crystal data and a summary of the intensity data collection parameters of compound **4** are provided in Tables 1 and 2, respectively. Similar to compound **3**, compound **4** lay on a crystallographic reflection plane and thus exhibited rigorously imposed reflection symmetry. A number of atoms, namely Al(1), N(1), C(13), C(2), C(1), B(9), and B(12), lay on the symmetry plane. Similar to compound **3**, the dimethylamine group of the *o*-carboranyl ligand was coordinated to the aluminum metal in complex **4**, resulting in the formation of a five-membered chelate ring, N(1)–Al(1)–C(1)–C(2)–C(13). The Al(1), C(15), C(15)*, and C(1) moieties were close to planar, with aluminum −0.435(4) Å above the C(15)C(15)*C(1) plane. The geometry of **4** was similar to that of **3** owing to the use of intramolecularly coordinated aluminum metal as a Lewis acid and a nitrogen atom as an electron donor. This tetrahedral distortion, with nearly "normal" angles [C(15)–Al(1)–N(1) 109.1(2)° and C(15)–Al(1)–C(1) 113.1(2)°] and a significantly different angle [C(1)–Al(1)–N(1) 88.4(2)°], is caused by the transannular Al–N interaction. The Al(1)–N(1) distance (2.090(5) Å) is in agreement with the corresponding values observed in $[(AlMe_3)_3]_4$[N-tetramethylcyclam] (2.093(3) Å) [44], $(Me_3Al)_2[(Me_2N)_2CH_2]$ (2.104(2), 2.112(2) Å) [56], and $Me_3Al{\cdot}NMe_3$ (2.099(1) Å) [43], but is longer than the sum of the covalent radii for Al and N (1.95 Å) [51]. The Al(1)–C(1) distance (2.010(6) Å) is slightly longer than the other two Al–C distances (Al(1)–C(15) and Al(1)–C(15)*, 1.947(5) Å). The Al–C distances of the Me_2Al group were similar to those of Me_3Al in the gas phase [43–57].

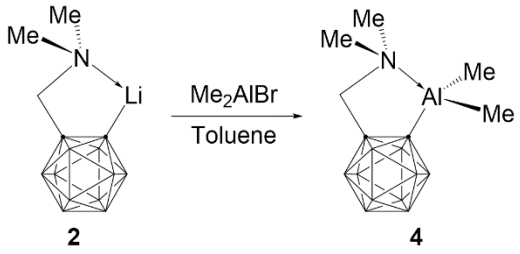

Scheme 2. Synthesis of $Cab^{N}AlMe_2$ (**4**).

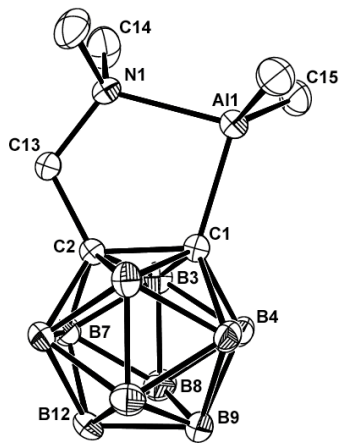

Figure 2. Molecular structure of $Cab^{N}AlMe_2$ (**4**). The thermal ellipsoids are drawn at the 30% probability level. (CCDC No. 2256553).

*3.3. Reaction of Cab^{N}AlBr$_2$ (**3**) with LiMe*

Compound **4** can be synthesized via another route using compound **3** (Scheme 3). When compound **3** and MeLi, a Lewis base, are reacted in a 1:2 ratio, compound Cab^{N}A1Me$_2$ (**4**) is obtained through a process of dimethylation. According to Scheme 1, the two bromine atoms of compound **3** can be selectively replaced by Lewis bases to produce compound **4**. However, compared to the yield obtained when reacting with Me_2AlBr and **2**, it was confirmed that the reaction between compound **3** and MeLi generated a very low yield. This result confirmed that compound **3** is easily decomposed in further reactions with Lewis bases such as pyridine, alkyl alcohol, and arylamine (Scheme 3), unlike previously reported gallium compounds. This is probably because compound **3** is more unstable than the gallium compound owing to the strong Lewis acid properties of aluminum [58–60]. When the ^{1}H and ^{13}C NMR spectra of this product were compared with those derived from **4**, it was confirmed that they were identical.

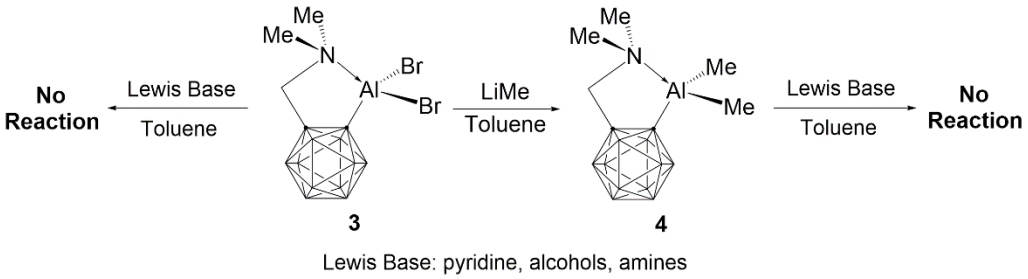

Scheme 3. Reaction of Cab^{N}AlBr$_2$ (**3**) with 2 equiv. of LiMe.

4. Conclusions

In summary, we prepared new types of 2-(dimethylaminomethyl-*o*-carboranyl) aluminum bromide and -dimethylaluminum complexes. A combination of X-ray crystallographic and spectroscopic studies, including IR, ^{1}H, ^{11}B, and ^{13}C NMR spectroscopy, confirmed the nature of these compounds. The X-ray crystallographic studies of complexes **3** and **4** provided the first structural data obtained on intramolecularly C,N-coordinated *o*-carboranylamino aluminum complexes. In compounds **3** and **4**, unlike gallium compounds, aluminum atoms preferred only the tetracoordinate by the C,N-chelate ligand in the molecule. However, *o*-carboranyl C,N-chelating ligands stabilized aluminum compounds, at least in inert environments, and showed the potential for isolation as a well-defined monomeric species. The intramolecular coordination of the N atom of the *o*-carboranyl ligand and the Al metal center has a significant effect on the stability of the starting materials, aluminum tribromide and dimethylaluminum bromide. This may have been be a result of changes in the electronic properties and bond strength of Al–C and Al–N owing to the C,N-chelation effect. In this study, unlike previous studies, it was confirmed that compounds **3** and **4** did not form a pentacoordinate compound when reacted with a strong Lewis base such as pyridine, but were easily decomposed due to the strong Lewis acidity of aluminum.

Supplementary Materials: The following supporting information can be downloaded at https://www.mdpi.com/article/10.3390/cryst13060877/s1, Tables S1–S6: Detailed information on the structural determinations and structural features of compounds **3** and **4** are provided in the Supplementary Materials.

Author Contributions: Conceptualization, J.-D.L. and H.S.; Designed and performed X-ray crystallography, J.-D.L.; Chemical experiments, J.-D.L.; Data Curation, J.-D.L. and H.S.; Writing—Original Draft Preparation, J.-D.L.; Writing—Review and Editing, J.-D.L. and H.S.; Supervision, J.-D.L.; Project Administration, J.-D.L.; Funding Acquisition, J.-D.L. All authors have read and agreed to the published version of the manuscript.

Funding: This research received no external funding.

Data Availability Statement: Crystallographic data for the structure of compounds **3** and **4** were deposited with the Cambridge Crystallographic Data Centre (CCDC No. 2256552 and 2256553). These data can be obtained free of charge via www.ccdc.cam.ac.uk/conts/retrieving.html) and the Supplementary Materials contains detailed crystallographic data (bond lengths, angles, and torsion angles) for compounds **3** and **4**.

Acknowledgments: This work was supported by the Basic Science Research Program through the National Research Foundation of Korea (NRF) funded by the Ministry of Education (2022R1F1A1074095).

Conflicts of Interest: The authors declare no conflict of interest.

Appendix A

CCDC 2256552 and 2256553 contain the supplementary crystallographic data of **3** and **4** for this paper. These data can be obtained free of charge via www.ccdc.cam.ac.uk/conts/retrieving.html (or from the Cambridge Crystallographic Data Centre, 12, Union Road, Cambridge CB2 1EZ, UK; Fax: +44 1223 336033; or deposit@ccdc.cam.ac.uk). Additional Supporting Information may be found online in the supporting information tab for this article.

References

1. Jastrzebski, J.T.B.H.; van Koten, G. Intramolecular Coordination in Organotin Chemistry. *Adv. Organomet. Chem.* **1993**, *35*, 241–294.
2. Schumann, H.; Hartmann, U.; Wassermann, W.; Dietrich, A.; Görlitz, F.H.; Pohl, L.; Hostalek, M. Intramolecularly Stabilized Organoaluminium, -gallium and -indium Derivatives Crystal Structures of {*o*-[(Dimethylamino)methyl]phenyl}dimethylgallium and *(o*-[(Diethylamino)methyl]pheny1)dimethylindium. *Chem. Ber.* **1990**, *123*, 2093–2099. [CrossRef]
3. Matsumoto, T.; Takamine, H.; Tanaka, K.; Chujo, Y. Synthesis and Characterization of Heterofluorenes with Five-coordinated Group 13 Elements. *Chem. Lett.* **2015**, *44*, 1658–1660. [CrossRef]
4. Zheng, W.; Roesky, H.W.; Mösch-Zanetti, N.C.; Schmidt, H.-G.; Noltemeyer, M. Synthesis and Characterization of Derivatives of a Chelating Aluminum Dichloride Complex Containing a 3,5-Di-*tert*-butylpyrazolato Unit. *Eur. J. Inorg. Chem.* **2002**, *2002*, 1056–1059. [CrossRef]
5. Kumar, R.; Rahbarnoohi, H.; Heeg, M.J.; Dick, D.G.; Oliver, J.P. Synthesis and Spectroscopic Investigations of Organoaluminum Derivatives of ((Dimethylamino)methyl)ferrocene. Crystal and Molecular Structures of $Me_3Al{\cdot}N(Me_2)CH_2C_5H_4FeCp$ and $[(2\text{-}C_4H_3S)_2Al{\cdot}N(Me_2)CH_2C_5H_4FeCp]_2O$. *Inorg. Chem.* **1994**, *33*, 1103–1108. [CrossRef]
6. Contreras, L.; Cowley, A.H.; Gabbaï, F.P.; Jones, R.A.; Carrano, C.J.; Bond, M.R. An intramolecularly base-stabilized monomeric organoaluminum dihydride. *J. Organomet. Chem.* **1995**, *489*, C1–C3. [CrossRef]
7. Isom, H.S.; Cowley, A.H.; Decken, A.; Sissingh, F.; Corbelin, S.; Lagow, R.J. Group 13 Halides and Hydrides with *o*-(Aminomethyl)phenyl Substituents. *Organometallics* **1995**, *14*, 2400–2406. [CrossRef]
8. Tian, X.; Woski, M.; Lustig, C.; Pape, T.; Fröhlich, R.; Le Van, D.; Bergander, K.; Mitzel, N.W. *N,N*-Diisopropylaminomethyllithium: Synthesis, Oxidative Degradation, and Organoaluminum and -gallium Derivatives. *Organometallics* **2005**, *24*, 82–88. [CrossRef]
9. Cowley, A.H.; Gabbaï, F.P.; Isom, H.S.; Decken, A. New developments in the chemistry of organoaluminum and organogallium hydrides. *J. Organomet. Chem.* **1995**, *500*, 81–88. [CrossRef]
10. Holtrichter-Rößmann, T.; Rösener, C.; Hellmann, J.; Uhl, W.; Würthwein, E.-U.; Fröhlich, R.; Wibbeling, B. Generation of Weakly Bound Al−N Lewis Pairs by Hydroalumination of Ynamines and the Activation of Small Molecules: Phenylethyne and Dicyclohexylcarbodiimide. *Organometallics* **2012**, *31*, 3272–3283. [CrossRef]
11. Aders, N.; Keweloh, L.; Pleschka, D.; Hepp, A.; Layh, M.; Rogel, F.; Uhl, W. P−H Functionalized Al/P-Based Frustrated Lewis Pairs in Dipolar Activation and Hydrophosphination: Reactions with CO_2 and SO_2. *Organometallics* **2019**, *38*, 2839–2852. [CrossRef]
12. Wong, E.W.Y.; Dange, D.; Fohlmeister, L.; Hadlington, T.J.; Jones, C. Extremely Bulky Amido and Amidinato Complexes of Boron and Aluminium Halides: Synthesis and Reduction Studies. *Aust. J. Chem.* **2013**, *66*, 1144–1154. [CrossRef]
13. Briegleb, F.; Geuther, A. Ueber das Stickstoffmagnesium und die Affinitäten des Stickgases zu Metallen. *Justus Liebigs Ann. Chem.* **1862**, *123*, 228–241. [CrossRef]
14. Hickman, A.L.; Chaudhuri, R.; Bader, S.J.; Nomoto, K.; Li, L.; Hwang, J.C.M.; Xing, H.G.; Jena, D. Next generation electronics on the ultrawide-bandgap aluminum nitride platform. *Semicond. Sci. Technol.* **2021**, *36*, 044001. [CrossRef]
15. Gong, J.; Zhou, J.; Wang, P.; Kim, T.-H.; Lu, K.; Min, S.; Singh, R.; Sheikhi, M.; Abbasi, H.N.; Vincent, D.; et al. Synthesis and Characteristics of Transferrable Single-Crystalline AlN Nanomembranes. *Adv. Electron. Mater.* **2023**, *9*, 2201309–2201317. [CrossRef]
16. Sang, X.; Wang, Y.; Wang, Q.; Zou, L.; Ge, S.; Yao, Y.; Wang, X.; Fan, J.; Sang, D. A Review on Optoelectronical Properties of Non-Metal Oxide/Diamond-Based p-n Heterojunction. *Molecules* **2023**, *28*, 1334–1347. [CrossRef]

17. Hite, J.K. A Review of Homoepitaxy of III-Nitride Semiconductors by Metal Organic Chemical Vapor Deposition and the Effects on Vertical Devices. *Crystals* **2023**, *13*, 387–398. [CrossRef]
18. Pinto, R.M.R.; Gund, V.; Dias, R.A.; Nagaraja, K.K.; Vinayakumar, K.B. CMOS-Integrated Aluminum Nitride MEMS: A Review. *J. Microelectromech. Syst.* **2022**, *31*, 500–523. [CrossRef]
19. Khan, S.; Angeles, F.; Wright, J.; Wishwakarma, V.; Ortiz, V.H.; Guzman, E.; Kargar, F.; Balandin, A.A.; Smith, D.J.; Jena, D.; et al. Properties for Thermally Conductive Interfaces with Wide Band Gap Materials. *ACS Appl. Mater. Interfaces* **2022**, *14*, 36178–36188. [CrossRef]
20. Wu, H.; Zhang, K.; He, C.; He, L.; Wang, Q.; Zhao, W.; Chen, Z. Recent Advances in Fabricating Wurtzite AlN Film on (0001)-Plane Sapphire Substrate. *Crystals* **2022**, *12*, 38–67. [CrossRef]
21. Zhao, S.; Mi, Z. Recent Advances on p-Type III-Nitride Nanowires by Molecular Beam Epitaxy. *Crystals* **2017**, *7*, 268–284. [CrossRef]
22. Giannazzo, F.; Fisichella, G.; Greco, G.; La Magna, A.; Roccaforte, F.; Pecz, B.; Yakimova, R.; Dagher, R.; Michon, A.; Cordier, Y. Graphene integration with nitride semiconductors for high power and high frequency electronics. *Phys. Status Solidi A* **2017**, *214*, 1600460–1600475. [CrossRef]
23. Ito, T. *Springer International Publishing AG, Part of Springer Nature 2018*; Matsuoka, T., Kangawa, Y., Eds.; Springer Series in Materials Science; Springer: Berlin/Heidelberg, Germany, 2018; Volume 269, pp. 1–5.
24. Stolyarchuk, N.; Markurt, T.; Courville, A.; March, K.; Zúñiga-Pérez, J.; Vennéguès, P.; Albrecht, M. Intentional polarity conversion of AlN epitaxial layers by oxygen. *Sci. Rep.* **2018**, *8*, 14111–14118. [CrossRef] [PubMed]
25. Wines, D.; Ersan, F.; Ataca, C. Engineering the Electronic, Thermoelectric, and Excitonic Properties of Two-Dimensional Group-III Nitrides through Alloying for Optoelectronic Devices ($B_{1-x}Al_xN$, $Al_{1-x}Ga_xN$, and $Ga_{1-x}In_xN$). *ACS Appl. Mater. Interfaces* **2020**, *12*, 46416–46428. [CrossRef]
26. Dai, X.; Hua, Q.; Sha, W.; Wang, J.; Hu, W. Piezo-phototronics in quantum well structures. *J. Appl. Phys.* **2022**, *131*, 010903–010917. [CrossRef]
27. Lenka, T.R.; Panda, A.K. Role of Nanoscale AlN and InN for the Microwave Characteristics of AlGaN/(Al,In)N/GaN-based HEMT. *Semiconductors* **2011**, *45*, 1211–1218. [CrossRef]
28. Shur, M. Physics of GaN-based Power Field Effect Transistors. *ECS Trans.* **2013**, *50*, 129–138. [CrossRef]
29. Aidam, R.; Diwo, E.; Godejohann, B.-J.; Kirste, L.; Quay, R.; Ambacher, O. Growth model investigation for AlN/Al(Ga)InN interface growth by plasma-assisted molecular beam epitaxy for high electron mobility transistor applications. *Phys. Status Solidi A* **2014**, *211*, 2854–2860. [CrossRef]
30. Freitas, J.A., Jr.; Gulbertson, J.C.; Glaser, E. Characterization of Defects in GaN: Optical and Magnetic Resonance Techniques. *Crystals* **2022**, *12*, 1294–1316. [CrossRef]
31. Parasad, S.; Islam, A. Characterization of AlInN/GaN based HEMT for Radio Frequency Applications. *Micro Nanosyst.* **2023**, *15*, 55–64.
32. Xu, R.L.; Rojo, M.M.; Islam, S.M.; Sood, A.; Vareskic, B.; Katre, A.; Mingo, N.; Goodson, K.E.; Xing, H.G.; Jena, D.; et al. Thermal conductivity of crystalline AlN and the influence of atomic-scale defects. *Appl. Phys.* **2019**, *126*, 185105–185111. [CrossRef]
33. Beall, H. *Boron Hydride Chemistry*; Muetterties, E., Ed.; Academic Press: New York, NY, USA, 1975; Chapter 9.
34. Lee, J.-D.; Baek, C.-K.; Ko, J.; Park, K.; Cho, S.; Min, S.-K.; Kang, S.O. Syntheses and Crystal Structures of Intramolecularly Stabilized Organogallium Compounds Containing an *o*-Carboranyl C,N-Chelating Ligand System. *Organometallics* **1999**, *18*, 2189–2197. [CrossRef]
35. Lee, J.-D.; Kim, S.-J.; Yoo, D.; Ko, J.; Cho, S.; Kang, S.O. Synthesis and Reactivity of Intramolecularly Stabilized Organotin Compounds Containing the C,N-Chelating *o*-Carboranylamino Ligand [*o*-$C_2B_{10}H_{10}(CH_2NMe_2)$-*C*,*N*]$^-$ ($Cab^{C,N}$). X-ray Structures of ($Cab^{C,N}$)SnR_2X (R = Me, X = Cl; R = Ph, X = Cl), ($Cab^{C,N}$)$_2$Hg, and [($Cab^{C,N}$)$SnMe_2$]$_2$. *Organometallics* **2000**, *19*, 1695–1703.
36. Lee, J.-D.; Ko, J.; Cheong, M.; Kang, S.O. Syntheses and Crystal Structures of Intramolecularly Stabilized Organo Aluminum, Gallium, and Indium Compounds Containing the *C*,*P*-Chelating *o*-Carboranylphosphino Ligand [*o*-$C_2B_{10}H_{10}(CH_2PMe_2)$-*C*,*P*]$^-$ ($Cab^{C,P}$). X-ray Structure of Pentacoordinated Group 13 Metal Complexes ($Cab^{C,P}$)$_2$MX (M = Ga, In; X = Cl). *Organometallics* **2005**, *24*, 5845–5852.
37. Heying, T.L.; Ager, J.W., Jr.; Clark, S.L.; Mangold, D.J.; Goldstein, H.L.; Hillman, M.; Polak, R.J.; Szymanski, J.W. A New Series of Organoboranes. I. Carboranes from the Reaction of Decaborane with Acetylenic Compounds. *Inorg. Chem.* **1963**, *2*, 1089–1092. [CrossRef]
38. Grosse, A.V.; Mavity, J.M. ORGANOALUMINUM COMPOUNDS. I. Methods of Preparation. *J. Org. Chem.* **1940**, *5*, 106–121. [CrossRef]
39. *SMART V5.05*; Software for the CCD Dector System. Bruker Analytical X-ray Systems, Inc.: Madison, WI, USA, 1998.
40. *SAINTPLUS, V5.00*; Software for the CCD Dector System. Bruker Analytical X-ray Systems, Inc.: Madison, WI, USA, 1998.
41. SADABS. Program for absorption correction using SMART CCD based on the method of: Blessing, R.H. *Acta Crystallogr.* **1995**, *A51*, 33.
42. *SHELXTL, Version 5.03*, Siemens Industrial Automation, Inc.: Madison, WI, USA, 1994.
43. Anderson, G.A.; Forgaard, F.R.; Haaland, A. On the Molecular Structure of the Complex Trimethylaluminium-Trimethylamine, $(CH_3)_3AlN(CH_3)_3$. *Acta Chem. Scand.* **1972**, *26*, 1947–1954. [CrossRef]

44. Robinson, G.H.; Zhang, H.; Atwood, J.L. Reaction of trimethylaluminum with a macrocyclic tetradentate tertiary amine. Synthesis and molecular structure of $[Al(CH_3)_3]_4$[N-tetramethylcyclam]. *J. Organomet. Chem.* **1987**, *331*, 153–160. [CrossRef]
45. Atwood, J.L.; Bennett, F.R.; Elms, F.M.; Jones, C.; Raston, C.L.; Robinson, K.D. Tertiary Amine Stabilized Dialane. *J. Am. Chem. Soc.* **1991**, *113*, 8183–8185. [CrossRef]
46. Atwood, J.L.; Bennett, F.R.; Jones, C.; Koutsantonis, G.A.; Raston, C.L.; Robinson, K.D. Polydentate Tertiary Amine Aluminium Hydride Adducts: Monomeric *versus* Polymeric Species. *J. Chem. Soc. Chem. Commun.* **1992**, *v*, 541–543. [CrossRef]
47. Atwood, J.L.; Jones, C.; Raston, C.L.; Robinson, K.D. The First Structural Characterization of a Five Coordinate Aluminum Trichloride-Bidentate Tertiary Amine Adduct, Trichloro (1,4-dimethylpiperazine) aluminum (III). *Main Group Chem.* **1996**, *1*, 345–347. [CrossRef]
48. Andrews, P.C.; Gardiner, M.G.; Raston, C.L.; Tolhurst, V.-A. Structural aspects of tertiary amine adducts of alane and gallane. *Inorg. Chim. Acta* **1997**, *259*, 249–255. [CrossRef]
49. Alexander, S.G.; Cole, M.L.; Forsyth, C.M. Tertiary Amine and N-Heterocyclic Carbene Coordinated Haloalanes—Synthesis, Structure, and Application. *Chem. Eur. J.* **2009**, *15*, 9201–9214. [CrossRef] [PubMed]
50. Carmalt, C.J.; King, S.J.; Mileham, J.D.; Sabir, E.; Tocher, D.A. Organoaluminum Silylamido Complexes. *Organometallics* **2004**, *23*, 2939–2943. [CrossRef]
51. Bondi, A. van der Waals Volumes and Radii. *J. Phys. Chem.* **1964**, *68*, 441–451. [CrossRef]
52. Evans, W.J.; Chamberlain, L.R.; Ziller, J.W. Synthesis and X-ray Crystal Structure of a Heterobimetallic Ethyl-Bridged Organoaluminum Complex: $(C_5Me_5)_2Sm(\mu\text{-}C_2H_5)_2Al(C_2H_5)_2$. *J. Am. Chem. Soc.* **1987**, *109*, 7209–7211. [CrossRef]
53. Li, X.-W.; Su, J.; Robinson, G.H. Synthesis, molecular structure, and reactivity of an Li_2Br_4 octahedrally stabilized organoaluminium bromide dimer. *Chem. Commun.* **1998**, *v*, 1281–1282. [CrossRef]
54. Cui, C.; Roesky, H.W.; Noltemeyer, M.; Schmidt, H.-G. Synthesis of Organoaluminum Chalcogenides $[RAl(\mu\text{-}E)]_2$ (R = $N(SiMe_3)C(Ph)C(SiMe_3)_2$, E = Se, Te) from Aluminum Dihydride $[RAlH(\mu\text{-}H)]_2$. *Organometallics* **1999**, *18*, 5120–5123. [CrossRef]
55. Hatop, H.; Roesky, H.W.; Labahn, T.; Fischer, A.; Schmidt, H.-G.; Noltemeyer, M. Syntheses and Structures of New Organoaluminum Fluorides. *Organometallics* **2000**, *19*, 937–940. [CrossRef]
56. Mitzel, N.W.; Lustig, C.Z. Organoaluminium and -gallium Lewis-Acid Adducts of Tetramethylmethylenediamine. *Zeitsch. Naturforsch.* **2004**, *59B*, 1532–1539. [CrossRef]
57. Almenningen, A.; Halvorsen, S.; Haaland, A. The Molecular Structure of Trimethylaluminium Monomer. *Chem. Commun.* **1969**, *12*, 644. [CrossRef]
58. Timoshkin, A.Y.; Bodensteiner, M.; Sevastianova, T.N.; Lisovenko, A.S.; Davydova, E.I.; Scheer, M.; Graßl, C.; Butlak, A.V. Do Solid-State Structures Reflect Lewis Acidity Trends of Heavier Group 13 Trihalides? Experimental and Theoretical Case Study. *Inorg. Chem.* **2012**, *51*, 11602–11611. [CrossRef] [PubMed]
59. Mück, L.A.; Timoshkin, A.Y.; Frenking, G. Design of Neutral Lewis Superacids of Group 13 Elements. *Inorg. Chem.* **2012**, *51*, 640–646. [CrossRef] [PubMed]
60. Estager, J.; Oliferenko, A.A.; Seddon, K.R.; Swadźba-Kwaśny, M. Chlorometallate(III) ionic liquids as Lewis acidic catalysts—A quantitative study of acceptor properties. *Dalton Trans.* **2010**, *39*, 11375–11382. [CrossRef]